Functional Diversity of Human Protection of Telomeres 1 Isoforms in Telomere Protection and Cellular Senescence

Qin Yang,[1] Ran Zhang,[1] Izumi Horikawa,[1] Kaori Fujita,[1] Yalda Afshar,[1] Antti Kokko,[2] Päivi Laiho,[2] Lauri A. Aaltonen,[2] and Curtis C. Harris[1]

[1]Laboratory of Human Carcinogenesis, Center for Cancer Research, National Cancer Institute, NIH, Bethesda, Maryland and [2]Molecular and Cancer Biology Research Program and Department of Medical Genetics, Biomedicum Helsinki, University of Helsinki, Helsinki, Finland

Abstract

Protection of telomeres 1 (POT1) proteins in various organisms bind telomeres and regulate their structure and function. In contrast to mice carrying two distinct *POT1* genes encoding two POT1 proteins (POT1a and POT1b), humans have the single *POT1* gene. In addition to full-length POT1 protein (variant v1), the human *POT1* gene encodes four other variants due to alternative RNA splicing (variants v2, v3, v4, and v5), whose functions are poorly understood. The functional analyses of the NH_2-terminally and COOH-terminally truncated POT1 variants in this study showed that neither the single-stranded telomere-binding ability of the NH_2-terminal oligonucleotide-binding (OB) folds nor the telomerase-dependent telomere elongation activity mediated by the COOH-terminal TPP1-interacting domain was telomere protective by itself. Importantly, a COOH-terminally truncated variant (v5), which consists of the NH_2-terminal OB folds and the central region of unknown function, was found to protect telomeres and prevent cellular senescence as efficiently as v1. Our data revealed mechanistic and functional differences between v1 and v5: (*a*) v1, but not v5, functions through the maintenance of telomeric 3′ overhangs; (*b*) p53 is indispensable to v5 knockdown-induced senescence; and (*c*) v5 functions at only a fraction of telomeres to prevent DNA damage signaling. Furthermore, v5 was preferentially expressed in mismatch repair (MMR)-deficient cells and tumor tissues, suggesting its role in chromosome stability associated with MMR deficiency. This study highlights a human-specific complexity in telomere protection and damage signaling conferred by functionally distinct isoforms from the single *POT1* gene. [Cancer Res 2007;67(24):11677–86]

Introduction

Telomeres are a specialized structure at chromosome ends consisting of tandem repetitive DNA sequence [(TTAGGG)n in humans] and the associated proteins. The very end of telomeric DNA is a single-stranded 3′ overhang (~75–300 bases in humans) of the (TTAGGG)n sequence, which plays a key role in the protection of telomeres from the degradation and fusion events as well as in the formation of the "t-loop" structure (1, 2). Telomere dysfunction associated with the loss of telomeric 3′ overhangs, induced by cellular stress, replicative exhaustion, or chemical treatment, can lead to the inhibition of cell proliferation (3, 4). Dysfunctional telomeres can also be a substrate for nonhomologous end joining, leading to chromosome end-to-end fusions, anaphase bridge formation, and global genome instability (5, 6). The structure and function of telomeres are regulated by a multiprotein complex containing single- and double-stranded telomere-binding proteins (termed "shelterin"; ref. 2) as well as by telomerase, a ribonucleoprotein enzyme that synthesizes telomeric DNA repeats (7). Protection of telomeres 1 (POT1), an evolutionarily conserved shelterin component, binds single-stranded telomeric DNA through the NH_2-terminal oligonucleotide-binding (OB) folds (2, 8). POT1 also interacts with TPP1 protein through the COOH-terminal region to take part in the shelterin complex (9–12). The full-length human POT1 protein reportedly functions to protect telomeric 3′ overhangs (13, 14), inhibit anaphase bridge formation (14, 15), maintain cell viability and proliferation (13–15), regulate telomerase and telomere length (11, 12, 16–19), define the recessed 5′ end of telomeres (13), and enhance the ability of WRN and BLM helicases to unwind telomeric DNA (20).

Mice have two POT1 proteins (POT1a and POT1b), which are encoded by two distinct genes that likely originated from a recent gene duplication event (21–23). Mouse POT1a and POT1b proteins seem to have overlapping and distinct functions in telomere protection and DNA damage signaling (21–23), providing functional diversity and complexity for telomere biology in this mammal. In contrast, humans have only one *POT1* gene. In addition to the full-length POT1 protein (also termed variant v1), at least four NH_2-terminally or COOH-terminally truncated isoforms (termed v2, v3, v4, and v5) are generated from the human *POT1* gene due to alternative RNA splicing (24). However, little is known about the functions of these truncated POT1 isoforms. Here, we examine an NH_2-terminally truncated variant (v4) and two COOH-terminally truncated variants (v2 and v5), as well as the full-length variant (v1), for their roles in telomere protection, telomere length regulation, and cellular senescence. This study provides novel insight into the dissection of functional domains of human POT1 protein and supports the notion that chromosome end protection and DNA damage signaling at human telomeres are cooperatively regulated by functionally distinct POT1 variants encoded by the single gene. The expression of a COOH-terminally truncated, telomere-protective variant may also contribute to chromosome stability in mismatch repair (MMR)-deficient tumors.

Note: Supplementary data for this article are available at Cancer Research Online (http://cancerres.aacrjournals.org/).

Current address for Q. Yang: Department of Radiation Oncology, Washington University School of Medicine in St. Louis, 4511 Forest Park Boulevard, St. Louis, MO 63108.

Requests for reprints: Curtis C. Harris, Laboratory of Human Carcinogenesis, Center for Cancer Research, National Cancer Institute, NIH, Building 37, Room 3068A, 37 Convent Drive, Bethesda, MD 20892-4258. Phone: 301-496-2048; Fax: 301-496-0497; E-mail: Curtis_Harris@nih.gov.

doi:10.1158/0008-5472.CAN-07-1390

Materials and Methods

Cells, lentiviral and retroviral vector transduction, and cellular senescence assays. A normal human fibroblast strain MRC-5 and human cancer cell lines used were obtained from the American Type Culture Collection. A normal human fibroblast strain WI-38 was from Coriell Cell Repository. NHF, a primary human fibroblast strain derived from foreskin, was previously described (25). HEC59 and HCT116 with a single copy of transferred, normal chromosomes 2 and 3, respectively, were gifts from Dr. Thomas Kunkel (National Institute of Environmental Health Sciences, Research Triangle Park, NC; refs. 26, 27). The lentiviral expression system was prepared by using the ViraPower lentiviral expression system (Invitrogen). Retroviral transduction followed the protocol recommended by Stratagene.[3] The examination of replicative life span and senescence-associated β-galactosidase (SA-β-Gal) staining in human fibroblasts were carried out as previously described (28).

Overexpression and short hairpin RNA knockdown vectors. The cloned cDNAs of POT1 variants v1, v2, and v5 were provided by Dr. Peter Baumann (Stowers Institute, Kansas City, MO; ref. 24). The Gateway cloning system (Invitrogen) was used to insert the cDNA in the lentiviral expression vector pLenti6/V5-DEST (Invitrogen) to drive the expression of each POT1 variant tagged with a "V5 epitope" at the COOH terminus (note that uppercase "V" is for this epitope tag, not for POT1 variants, in this article). To obtain the lentiviral expression vector of v4 (13), the initiation codon in the v1 expression vector was changed from ATG to CCG by site-directed mutagenesis. The lentiviral short hairpin RNA (shRNA) vectors used to knock down v1 and v5 expression (sh-v1 and sh-v5, respectively) were prepared at BioMarkers (shRNA sequences are available upon request). Note that the v5 target sequence is at the 3′ untranslated region of endogenous v5 mRNA and absent in the lentivirally overexpressed v5 mRNA (see Fig. 3*D*). A retroviral shRNA construct for p53 knockdown (29) was derived from pSUPERretro vector carrying a puromycin-resistant gene (OligoEngine). pLPC-Myc-TRF2$^{\Delta B\Delta M}$, a retroviral construct expressing a myc epitope-tagged, dominant-negative mutant of TTAGGG repeat factor (TRF) 2 (30), was a gift from Dr. Titia de Lange (Rockefeller University, New York, NY). The Flag-tagged TPP1 expression vector (9) was a gift from Dr. Zhou Songyang (Baylor College of Medicine, Houston, TX). The retroviral vector expressing human telomerase reverse transcriptase (hTERT) was previously described (31).

Anaphase bridge formation. Cells were fixed with 100% methanol at −20°C for 30 min and stained with the Prolong Gold antifade reagent with 4′,6-diamidino-2-phenylindole (DAPI; Invitrogen). At least 60 anaphase cells were examined for each sample per experiment. When one or more perpendicularly aligned connecting chromatin filaments were observed in a well-separated parallel anaphase, the anaphase was defined as positive for bridge formation.

Metaphase chromosome preparation and fluorescence *in situ* hybridization analysis. To arrest the cells at metaphase, 0.1 μg/mL colcemid (Invitrogen) was added to the culture 2 h before the harvest. The cells were treated in hypotonic solution (0.06 mol/L KCl) and fixed. The telomeric peptide nucleic acid (PNA) fluorescence *in situ* hybridization (FISH) assay was performed with the Telomere PNA FISH kit/Cy5 from Dako following the manufacturer's instructions. At least 100 well-spread metaphases in each group were examined for chromosome abnormalities (i.e., multicentric chromosomes, chromosome end joining, and breaks). The percentage of cells with chromosome abnormalities (mean ± SD) was obtained from three independent experiments.

Measurement of telomeric 3′ overhang, telomere length, and telomerase activity. Genomic DNA samples were digested with *Hin*fI and electrophoresed through 0.7% agarose gel. After drying, the gel was hybridized with ^{32}P-labeled $[CCCTAA]_4$ oligonucleotide as previously described (32) followed by washing and signal detection using the Typhoon 8600 system (Molecular Dynamics). The amounts of telomeric 3′ overhangs, normalized with loaded DNA amounts detected with ethidium bromide (EtBr) staining of the gel, were quantitated by using the ImageQuant version 5.2 software (Molecular Dynamics). After denaturation, the same procedures were repeated to examine telomere length, which was indicated as a peak terminal restriction fragment length. Telomerase activity was detected using the TRAPeze Telomerase Detection kit (Chemicon International).

Western blot, immunoprecipitation, and immunofluorescence. Western blot analyses and immunoprecipitation followed standard procedures as previously described (14, 28). Indirect immunofluorescence was performed as previously described (33). Antibodies used are as follows: anti-V5 epitope (Invitrogen), anti-myc epitope (Invitrogen), anti-Flag epitope (Sigma-Aldrich), anti-POT1 (Santa Cruz Biotechnology), anti-POT1 (Novus Biologicals), anti-p53 (DO-1, Santa Cruz Biotechnology), anti-phospho-p53 (Ser^{15}; Cell Signaling Technology), anti-p21^{WAF1} (Oncogene Sciences), anti-p16^{INK4A} (Santa Cruz Biotechnology), anti-β-actin (Abcam), anti-γ-H2AX (Upstate), anti-hRAP1 (Bethyl Laboratories), anti-TRF2 (Santa Cruz Biotechnology), anti-lamin A/C (Santa Cruz Biotechnology), Alexa Fluor 488–conjugated anti-mouse IgG (Molecular Probes), and Alexa Fluor 568–conjugated anti-rabbit IgG (Molecular Probes).

mRNA expression analyses. The real-time quantitative reverse transcription-PCR (RT-PCR) assays and the data analyses were performed as previously described (34). *Glyceraldehyde-3-phosphate dehydrogenase* (*GAPDH*) was used as the endogenous control gene (Applied Biosystems). For detection of v1, the Taqman predeveloped assay reagent for human POT1 (assay ID Hs00209984_m1, Applied Biosystems) was used. The primers and probe for v5 were synthesized at Applied Biosystems (shRNA sequences are available upon request). The conventional RT-PCR assay, which simultaneously detects the splicing variants encoding v1, v2, and v5 isoforms, was carried out using the platinum Taq kit (Invitrogen) and the following primer pair: TTCAGATGTTATCTGTCAATCAGAACCTG and ATGTATTGTTCCTTGTATAAGAAATGGTGC (24). Each PCR product was purified from an agarose gel followed by direct DNA sequencing. To specifically detect endogenous v5 mRNA, but not the lentivirally expressed v5, in the conventional RT-PCR, the following primers were used: CATCGGCTACAAAATCTG and ACCATTTTCTCTTGGTCTCAG (used in Fig. 3*D* and Supplementary Fig. S6).

Tumor tissue samples. The tumor tissue samples were collected from medical institutions in Finland (35, 36). The MMR status of the samples was determined using the microsatellite markers BAT25, BAT26, BAT40, D2S123, D17S250, D5S346, and D18S34. Hereditary nonpolyposis colorectal cancer (HNPCC) was diagnosed based on pathogenic germ-line *MLH1* and *MSH2* mutations. Patient information and samples were collected after obtaining informed consent. The study was approved by the appropriate ethics review committees.

Results

Overexpression of POT1v1 and POT1v5 inhibits anaphase bridge formation and chromosome abnormalities. To investigate the functions of human POT1 variants, we constructed the lentiviral overexpression vectors driving v1 (full length), v2 (retaining two NH_2-terminal OB folds and missing the COOH-terminal half), v4 (starting at Met^{132} and missing most of the first OB fold), and v5 (retaining two NH_2-terminal OB folds and missing most of the COOH-terminal TPP1-interacting region; Supplementary Fig. S1*A*), each fused in frame to a "V5 epitope tag" (uppercase V for this epitope tag and lowercase "v" for POT1 variants in this article). When an equal titer of vector supernatant (multiplicity of infection = 3) from each POT1 overexpression construct or a vector control was transduced to HT1080 cells, almost all of the cells became blasticidin S resistant and continued to proliferate, showing high transduction efficiency in this experimental system and no apparent effect on cell proliferation by overexpression of any POT1 variant. The expression of each variant in its expected molecular weight was detected by the anti-V5 epitope antibody and the anti-POT1 antibodies (Supplementary Fig. S1*B*).

[3] http://www.stratagene.com/manuals/217566.pdf

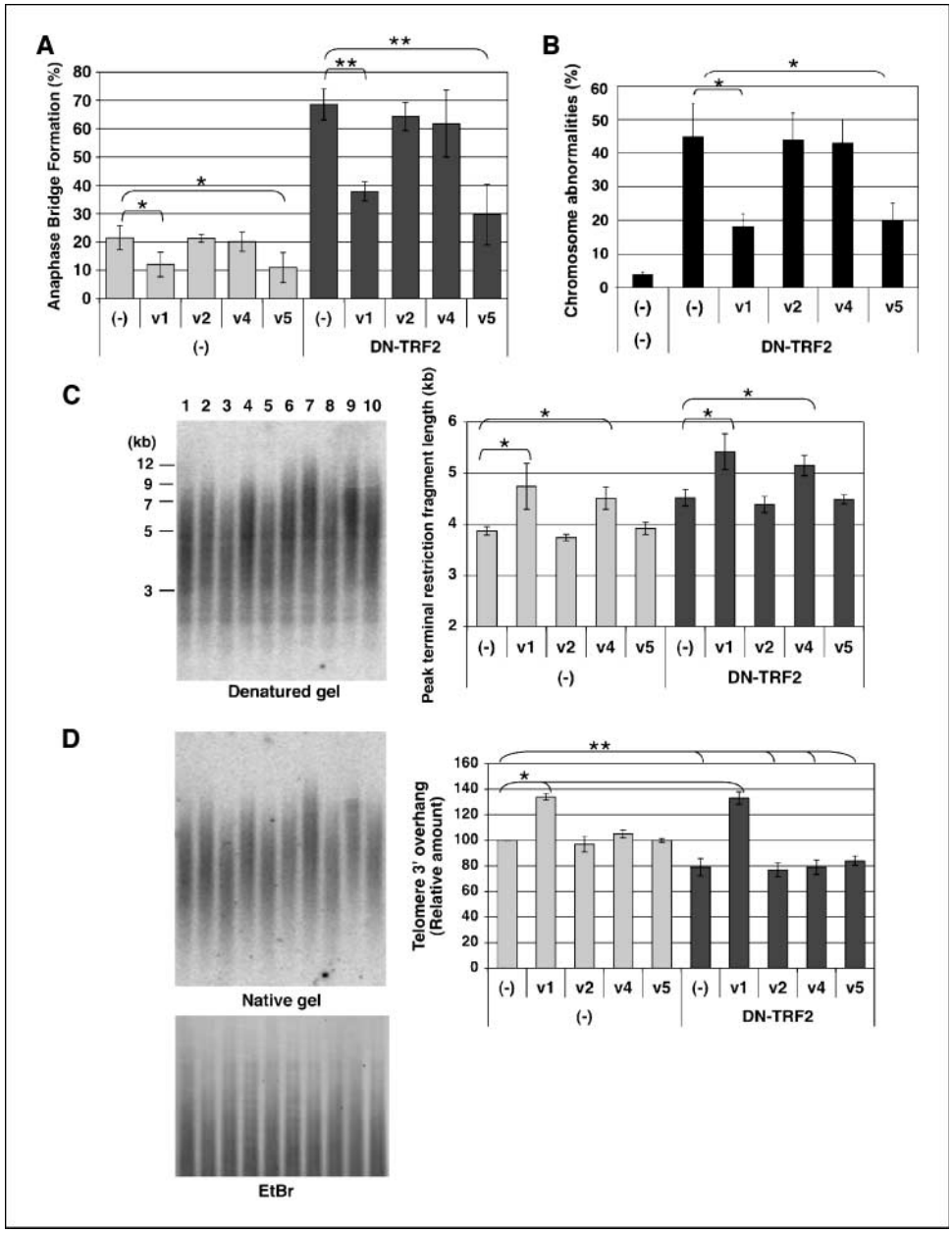

Figure 1. Human POT1 variants have different effects on anaphase bridge formation, telomere length, and telomeric 3′ overhang. *A,* anaphase bridge formation (number of anaphases with bridge formation/number of anaphases examined) in HT1080 cells overexpressing POT1 variants. Seven days after the lentiviral transduction of POT1 overexpression vectors, the cells were transduced with a control retroviral vector (−) or the retroviral vector expressing TRF2$^{\Delta B\Delta M}$ (*DN-TRF2*). Western blot, using anti-myc epitope antibody, confirmed similar levels of TRF2$^{\Delta B\Delta M}$ expression in all the transduced cells. Anaphase bridge formation was examined 5 d after the retroviral transduction. *Columns,* mean of three independent experiments; *bars,* SD. *, $P < 0.05$; **, $P < 0.001$. *B,* telomere FISH analysis of telomere dysfunction-induced chromosome abnormalities in HT1080 cells overexpressing POT1 variants. The lentiviral transduction of POT1 overexpression vectors followed by the retroviral transduction of TRF2$^{\Delta B\Delta M}$ (*DN-TRF2*) was performed as in *A*. Chromosome abnormalities were examined 5 d after the DN-TRF2 transduction. *Columns,* mean percentage of cells with chromosome abnormalities from three independent experiments; *bars,* SD. *, $P < 0.001$. *C* and *D,* genomic DNA was isolated from the same set of HT1080 cells at the same day as in *A*. *Lanes 1* to *5,* control retroviral vector; *lanes 6* to *10,* TRF2$^{\Delta B\Delta M}$ retroviral vector. *Lanes 1* and *6,* control lentiviral vector; *lanes 2* and *7,* v1 overexpression; *lanes 3* and *8,* v2 overexpression; *lanes 4* and *9,* v4 overexpression; *lanes 5* and *10,* v5 overexpression. The DNA samples were digested by *Hin*fI and analyzed in the in-gel hybridization with ^{32}P-[CCCTAA]$_4$ probe under denatured (*C*) or native (*D*) conditions. In *C*, the image analysis determined a peak in smear of telomere signals (peak terminal restriction fragment length). *, $P < 0.05$. In *D*, 3′ overhang signals were normalized with loaded DNA amounts (EtBr) and shown as the relative amounts to cells with both overexpression and shRNA vector controls (−/−). *, $P < 0.05$ (increase); **, $P < 0.05$ (decrease). *Columns,* mean of two independent experiments; *bars,* SD.

We examined the formation of anaphase bridges (Fig. 1*A*; Supplementary Fig. S2*A*), an indicator of telomere dysfunction and chromosome end-to-end fusions (5, 6), in these POT1 variant-expressing HT1080 cells (Fig. 1*A, left*). In vector control cells, 21% of anaphases showed bridge formation. Whereas the overexpression of v2 or v4 had no effect on anaphase bridge formation, decreased anaphase bridge formation was observed in v1- or v5-overexpressing HT1080 cells (12% or 11%, respectively). Under the condition where telomere dysfunction was experimentally induced by the dominant-negative mutant of TRF2 (TRF2$^{\Delta B\Delta M}$; ref. 30), the frequency of anaphase bridge formation remarkably increased up to ~70% in vector control cells (Fig. 1*A, right*). The overexpression of v1 and v5, but not v2 and v4, again strongly inhibited the TRF2$^{\Delta B\Delta M}$-induced anaphase bridge formation (38% and 30% in v1- and v5-expressing cells, respectively). Consistent with the ability to inhibit anaphase bridge formation, the overexpression of v1 and v5 resulted in a significant reduction in TRF2$^{\Delta B\Delta M}$-induced chromosome abnormalities (≤20% in v1- and v5-overexpressing cells versus >40% in control, v2- and v4-overexpressing cells; Fig. 1*B*), such as dicentric or multicentric chromosomes due to telomere dysfunction (Supplementary Fig. S2*B*).

Different activities of POT1 isoforms on telomere length and 3′ overhang. The POT1 variant-expressing HT1080 cells were examined for their telomeres in the in-gel hybridization experiments under denatured and native conditions. The measurement of telomere terminal restriction fragment length, an indicator of overall telomere length in the cells, in the denatured gel (Fig. 1*C*) showed that the overexpression of v1 and v4, but not v2 and v5, significantly elongated telomere length. This effect was likely telomerase dependent because it was not observed in telomerase-negative human fibroblasts (data not shown). With the expression of a dominant-negative TRF2 mutant (TRF2$^{\Delta B\Delta M}$) that increased

terminal restriction fragment length (30, 37), v1 and v4 further elongated telomeres. The ability of v1 and v4 to elongate telomere length was correlated with their ability to interact with TPP1 (Supplementary Fig. S3), consistent with the recent finding that the POT1-TPP1 complex enhances telomerase recruitment and processivity *in vitro* (11, 12).

The quantitation of amounts of single-stranded telomere repeat DNA in the native gel (Fig. 1*D*) showed that the overexpression of v1, but not the others, resulted in a significant increase in 3′ overhang. The expression of TRF2$^{\Delta B\Delta M}$ reduced the amount of 3′ overhang in vector control cells, which led to anaphase bridge formation, as previously reported (30). Whereas v2-, v4-, and v5-overexpressing cells underwent the decrease in 3′ overhang amounts similar to vector control cells, v1 overexpression made the cells resistant to the TRF2$^{\Delta B\Delta M}$-induced loss of 3′ overhangs.

Endogenous POT1v1, but not POT1v5, is critical to maintenance of 3′ overhang, but both contribute to telomere protection. To further investigate the roles of v1 and v5 in telomere protection, we used a lentiviral shRNA vector system to specifically knock down the expression of endogenous v1 or v5. Endogenous v1 expression was reduced by 60% to 70% in HT1080 and HCT116 cells transduced with the shRNA vector against v1 mRNA (sh-v1) but not in those with the shRNA vector against v5 mRNA (sh-v5; Fig. 2*A, left*). Similarly, ~60% suppression of v5 expression was observed in the cells with sh-v5, but not in the cells with sh-v1 (Fig. 2*A, right*). The v1 and v5 knocked down HT1080 cells both showed an increase in anaphase bridge formation (Fig. 2*B*), although the frequency (39% and 34%, respectively) was modest compared with the effect of TRF2 inhibition by TRF2$^{\Delta B\Delta M}$ (described above, Fig. 1*A*). HCT116 cells showed a much lower background level of anaphase bridges (<5% in scrambled shRNA control; discussed below). Both sh-v1 and sh-v5 resulted in an increased, but still modest, frequency of anaphase bridge formation in these cells (<15%). As shown in Fig. 2*C*, the amounts of 3′ overhangs in HT1080 and HCT116 with sh-v1 were reduced, whereas sh-v5 had no apparent effects on 3′ overhangs in these cells. The shRNA knockdown of v1 led to telomere length elongation (Fig. 2*D*).

Endogenous POT1v5, as well as POT1v1, protects normal human cells from cellular senescence. The shRNA knockdown of endogenous v1 or v5 induced cellular senescence, characterized by cell growth arrest and SA-β-Gal activity, in normal human fibroblast strains MRC-5 (Fig. 3*A*), NHF (see below, Fig. 4*B* and *C*), and WI-38 (Supplementary Fig. S4). The significant decrease in bromodeoxyuridine incorporation was associated with sh-v1–induced and sh-v5–induced senescence (1.9% and 2.0%, respectively, compared with 43.9% in control cells; Supplementary Fig. S5). The induction of cellular senescence by sh-v1 was associated with ~40% decrease in 3′ overhang amounts, consistent with the previous findings (13, 14), whereas senescent sh-v5 cells still maintained 3′ overhangs comparable with the control nonsenescent cells (Fig. 3*B*). No significant changes in overall telomere length were observed in MRC-5 fibroblasts with sh-v1 or sh-v5 (Fig. 3*C*). The lentiviral overexpression of v5 (which is not targeted by sh-v5; see Materials and Methods), but not the other variants, rescued the cells from sh-v5–induced cellular senescence (Fig. 3*D*), excluding the possibility of an off-target effect of sh-v5. Endogenous v5 expression was found to be down-regulated in senescent human fibroblasts (Supplementary Fig. S6), further supporting the physiologic importance of v5 in cellular replicative potential.

p53 is indispensable for cellular senescence by POT1v5 knockdown, but not by POT1v1 knockdown. The ectopic expression of telomerase may allow normal human cells to bypass cellular senescence (38). To examine whether sh-v1 and sh-v5 induce cellular senescence in the presence of the ectopically expressed telomerase, we used NHF-TERT cells, a human fibroblast cell line immortalized by a retroviral expression of *hTERT*, which express telomerase activity (Supplementary Fig. S7*A*) and have long telomeres (Supplementary Fig. S7*B*). As shown in Supplementary Fig. S7*C* and *D*, both sh-v1 and sh-v5 induced cellular senescence in NHF-TERT cells as efficiently as in primary NHF fibroblasts. Thus, telomerase expression or elongated telomeres do not compensate the inadequate levels of v1 and v5 in protecting normal human cells from cellular senescence.

To further investigate a mechanistic difference between v1 and v5 in cellular senescence, p53 expression was knocked down by a shRNA vector in a primary human fibroblast strain NHF. The resulting NHF-p53KD cells almost completely lost the induction of p53 protein in response to Adriamycin, a DNA-damaging agent (Fig. 4*A*). In the NHF-p53KD cells lacking a p53 response to DNA damage, sh-v1 induced cellular senescence as efficiently as it did in cells with a control vector (NHF-pSR; Fig. 4*B* and *C*). In marked contrast, the ability of sh-v5 to induce cellular senescence was abrogated in NHF-p53KD cells (Fig. 4*B* and *C*). The p53 dependence of sh-v5–induced senescence in this experiment was consistent with the Western blot results of cellular senescence-regulatory factors in normal human fibroblasts (WI-38 in Fig. 4*D* and MRC-5 in Supplementary Fig. S8). Both sh-v1 and sh-v5 led to the increase in Ser^{15}-phosphorylated p53 and the up-regulation of p21^{WAF1}, an effector of p53-mediated cellular senescence. In contrast, only sh-v1 induced the expression of p16^{INK4A}, another major effector for cellular senescence in human cells. These results suggest that, whereas both the p53 and the p16^{INK4A} pathways mediate sh-v1–induced senescence, sh-v5–induced senescence is mediated by the p53 pathway, but not by the p16^{INK4A} pathway.

Differential DNA damage foci formation by POT1v1 and POT1v5 knockdown. We examined the phosphorylated histone H2AX (γ-H2AX; ref. 25), an indicator of cellular DNA damage, in human fibroblasts (NHF and WI-38) that were induced to senesce by sh-v1 and sh-v5. The number of γ-H2AX foci detected by immunofluorescence (Fig. 5*A, green*, and *B*) and the amount of γ-H2AX in Western blot (Fig. 5*C*) remarkably increased in both sh-v1–induced and sh-v5–induced cellular senescence. Most of the γ-H2AX foci induced by sh-v1 (75–79%) were colocalized with the telomere proteins hRAP1 (39) and TRF2 (Fig. 5*A*; Supplementary Fig. S9; ref. 30), showing that the inhibition of endogenous v1 expression resulted in many dysfunctional telomeres recognized as DNA damage. In contrast, fewer sh-v5–induced γ-H2AX foci (16–19%) were colocalized with TRF2 and hRAP1 (Fig. 5*A*; Supplementary Fig. S9), suggesting that endogenous v5 also functions at sites other than telomeres. This notion was consistent with the immunofluorescence observation that v1 frequently colocalized with hRAP1 (Supplementary Fig. S10) and TRF2 (data not shown; refs. 14, 16, 24), whereas v5 showed only <20% colocalization (Supplementary Fig. S10; data not shown).

POT1v5 is preferentially expressed in MMR-deficient tumors. It is known that MMR-proficient tumors show chromosome instability, whereas MMR-deficient tumors do not (40). The lower frequency of anaphase bridge formation in HCT116 (MMR deficient; Fig. 2*B*) is consistent with chromosome stability in this cell line (40). The telomere-protective v5 was much more

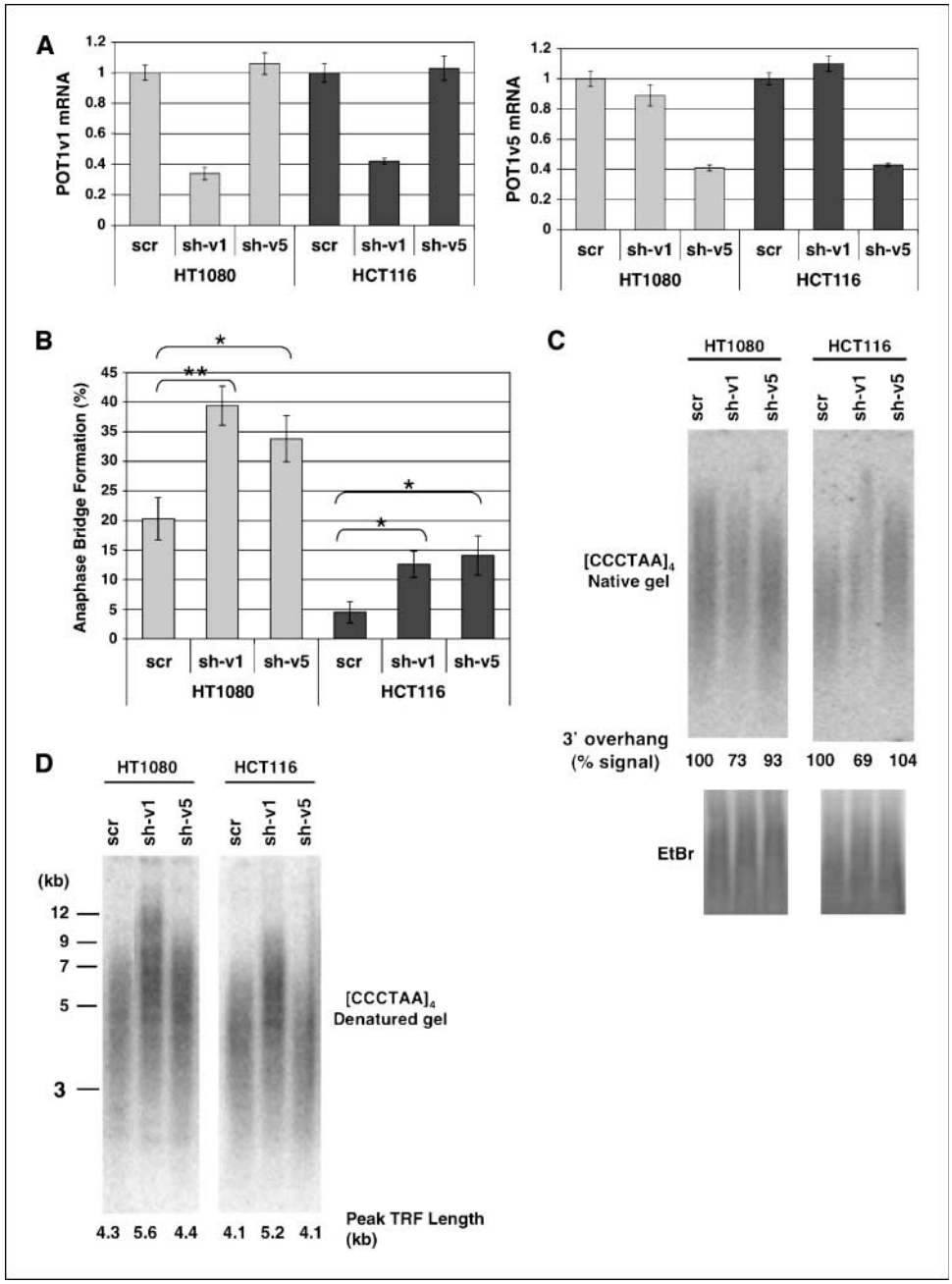

Figure 2. Endogenous POT1v1 and POT1v5 contribute to telomere protection in different manners. HT1080 and HCT116 cells were transduced with scrambled shRNA control (*scr*), shRNA targeting POT1v1 (*sh-v1*), or shRNA targeting POT1v5 (*sh-v5*). *A,* real-time quantitative RT-PCR assays of POT1v1 (*left*) and POT1v5 (*right*). For each cell line, the data (mean ± SD) are shown as relative values to the expression level in scrambled shRNA control. Note that the actual value of POT1v5 expression in HCT116 is ~10-fold higher than that in HT1080 (see Supplementary Fig. S11*A*). *B,* anaphase bridge formation was examined 10 d after the shRNA transduction. *Columns,* mean of two independent experiments; *bars,* SD. *, $P < 0.05$; **, $P < 0.01$. *C,* genomic DNAs were isolated 10 d after the shRNA transduction digested with *Hin*fI and were used in the in-gel hybridization with ^{32}P-[CCCTAA]$_4$ probe under native conditions as in Fig. 1*D*. The relative amounts of 3′ overhang (% signal to scrambled shRNA control cells) are shown. *D,* the same gels used in *C* were denatured and neutralized, and rehybridized with ^{32}P-[CCCTAA]$_4$ probe. The peak terminal restriction fragment lengths are shown below the pictures.

abundantly expressed in HCT116 than in HT1080 (Fig. 2*A* legend, Supplementary Fig. S11*A* and *B*); therefore, we examined whether the high expression of v5 is generally associated with MMR-deficient, chromosomally stable human tumors. The real-time quantitative RT-PCR (Supplementary Fig. S11*A*) and/or the conventional RT-PCR amplifying alternatively spliced mRNAs encoding the variants v1, v2, and v5 (Supplementary Fig. S11*B*; ref. 24) showed that three other MMR-deficient tumor cell lines (HEC59, HCT15, and RKO), but not four MMR-proficient cell lines (HeLa, 293, SW620, and HT29), expressed high levels of v5 mRNA. Interestingly, whereas v1 was abundantly expressed in all the cell lines, the detection of v2 was concomitant with that of v5. The examination of primary tumor tissues, including MMR-deficient colorectal cancers from HNPCC patients (8 cases), MMR-deficient (10 cases) and MMR-proficient (21 cases) sporadic colorectal cancers, and MMR-proficient lung cancers (8 cases), further supported the correlation between v5 expression and chromosome stability in MMR-deficient tumors (Supplementary Fig. S11*C*; Table 1). In all of the cases but one (c1021), the detection of v5 mRNA was concordant with the MMR-deficient status. The coupling of v2 and v5 expression was also common in these primary tissue samples with only one exception (case c1021, again).

Discussion

This study is the first detailed characterization of *in vivo* functions of human POT1 variants and presents novel, as well as confirmative, findings on telomere biology in human cells. Our data on the function of full-length human POT1 (variant v1), including telomere elongation, protection of 3′ overhangs,

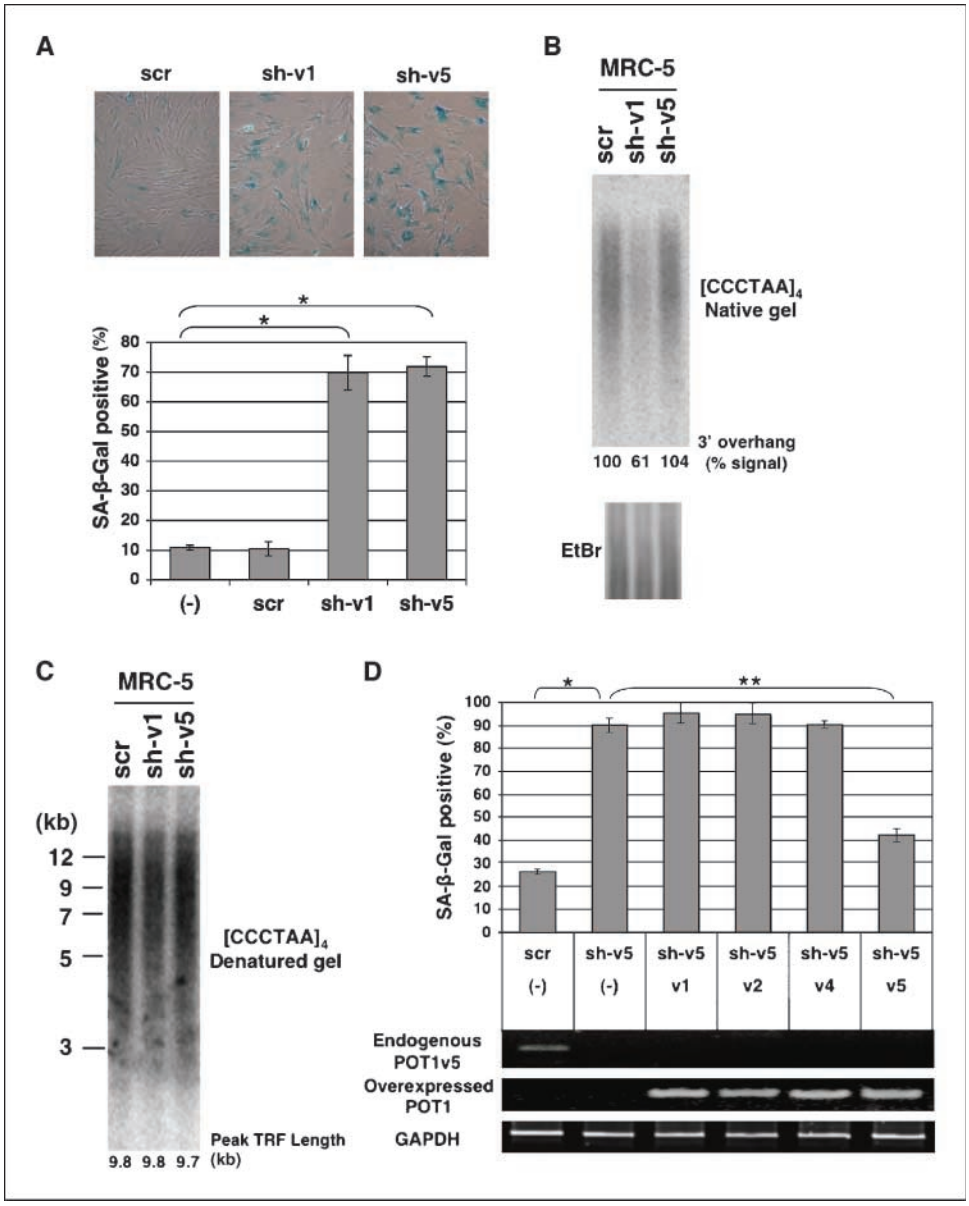

Figure 3. shRNA knockdown of endogenous POT1v1 or POT1v5 induces cellular senescence in human fibroblasts. *A,* normal human MRC-5 fibroblasts at passage 32 were transduced with scrambled shRNA control (*scr*), shRNA targeting POT1v1 (*sh-v1*), or shRNA targeting POT1v5 (*sh-v5*), as in Fig. 2. At 8 d after the transduction, cells were examined for SA-β-Gal activity. *Top,* representative pictures; *bottom, columns,* mean of two independent experiments; *bars,* SD. *(−),* untransduced MRC-5. *, $P < 0.0001$. *B* and *C,* genomic DNAs isolated 6 d after the shRNA transduction were digested by *Hin*fI and analyzed in the in-gel hybridization with ^{32}P-[CCCTAA]$_4$ probe under native (*B*) or denatured (*C*) conditions. The relative amounts of 3′ overhang (*B*) and the peak terminal restriction fragment lengths (*C*) are shown as in Fig. 2*C* and *D*, respectively. *D,* v5 overexpression rescues cellular senescence induced by shRNA knockdown of v5. MRC-5 fibroblasts at passage 41 were transduced with the lentiviral overexpression vector for v1, v2, v4, or v5 or a control vector (−). Five days later, the cells were transduced with the shRNA vector targeting v5 (*sh-v5*), cultured for 8 d further, and examined for SA-β-Gal activity. As a control, the cells transduced with control empty vector (−) and then with scrambled shRNA control (*scr*) were included in the assay. *Columns,* mean of two independent experiments; *bars,* SD. *, $P < 0.0001$; **, $P < 0.001$. *Bottom,* RT-PCR results of endogenous v5 mRNA, overexpressed POT1 variants (same assay as in Supplementary Fig. S1*B*), and GAPDH control.

inhibition of anaphase bridge formation and chromosome aberrations (Figs. 1 and 2), and protection from cellular senescence (Fig. 3), are consistent with the previous findings (13–15, 18), validating our experimental design and procedures. The functional analyses of NH_2-terminally or COOH-terminally truncated variants and the comparison with the full-length protein provide important insight into the dissection of functional domains of human POT1. v2, virtually consisting of only two OB folds, had no *in vivo* effects on telomere length, amounts of 3′ overhangs, and the formation of anaphase bridge and abnormal chromosomes (Fig. 1). The NH_2-terminally truncated v4 variant, missing an OB fold, failed to maintain 3′ overhangs and to inhibit anaphase bridge formation and chromosome aberrations (Fig. 1). These findings suggest that the intact NH_2-terminal OB folds are necessary, but not sufficient, for *in vivo* telomere protection functions of POT1. Consistently, our data also suggest that both the ability of the OB folds to bind single-stranded telomeric DNA (8, 24) and the participation in the shelterin complex through TPP1 interaction are necessary for efficient *in vivo* telomere localization of POT1 (Supplementary Figs. S3 and S10), in agreement with the *in vitro* biochemical data showing that POT1-TPP1 interaction enhances POT1 affinity for single-stranded telomeric DNA (11, 12).

Colgin et al. (18) suggested POT1 as a positive regulator of telomere length because of telomere elongation by POT1 overexpression, whereas Ye et al. (10) regarded it as a negative regulator of telomere length, because they observed that shRNA knockdown of POT1 resulted in telomere elongation. This study showed that either overexpression or shRNA knockdown of full-length POT1 (v1) resulted in telomere elongation in the same cell line (HT1080) under similar experimental settings (Figs. 1*C* and 2*D*). In both cases, the telomere elongation was likely to be dependent on telomerase activity, because it did not occur in telomerase-negative fibroblasts (Fig. 3*C*; data not shown). Our data provide *in vivo* evidence for dual roles of human POT1 in regulating telomerase function (i.e., negative regulation through preventing telomerase access to a ssDNA substrate and positive regulation by serving as a

telomerase processivity factor), which were suggested by *in vitro* biochemical studies (11, 12, 17, 19). We hypothesize that a certain level of POT1 expression is responsible for homeostatic control of telomere length in telomerase-expressing human cells and that a deviation of POT1 expression in either direction may shift the homeostasis toward a longer length of telomeres. Loayza and de Lange (16) showed that POT1(ΔOB), an artificial mutant lacking the first NH_2-terminal 126 residues, led to telomere elongation when overexpressed. In this study, the overexpression of v4, which is virtually identical to POT1(ΔOB), caused telomere elongation to the same extent as full-length POT1 (v1; Fig. 1*C*). It is likely that variant v4 and POT1(ΔOB), even without the first OB fold, still retain the ability of full-length POT1 to regulate telomere length in a telomerase-dependent manner. The interaction with TPP1 (Supplementary Fig. S3) seems essential for this telomerase-dependent telomere length regulation because TPP1 can directly associate with hTERT, the catalytic component of human telomerase enzyme (11). Our findings in the v4 overexpression and v1 knockdown experiments (Figs. 1 and 2) showed that elongated telomeres by themselves were not a primary determinant of the protected state of telomeres.

One of the major findings in this study is the biological activity of v5, which consists of two NH_2-terminal OB folds and a central region of unknown function and lacks the TPP1-binding ability (Supplementary Fig. S1*A* and S3). Despite the infrequent *in vivo* telomere localization of v5 similar to the nonfunctional v2 (Supplementary Fig. S10), v5 functioned to protect telomeres from end-to-end fusions (Figs. 1*A* and *B* and 2*B*) and prevent normal human cells from undergoing senescence (Fig. 3*A*) as effectively as the full-length v1. One interesting possibility is that v5 may bind and protect telomeres with a specific structure (e.g., a very short 3′ overhang), which are most susceptible to becoming dysfunctional. This notion is consistent with no overall change in 3′ overhang amounts and a few telomere-associated γ-H2AX foci induced by shRNA knockdown of v5 (Figs. 2*C*, 3*B*, and 5*A*; Supplementary Fig. S9). It is also possible that v5 competes and/or cooperates with the other single-stranded telomere-binding proteins, such as RPA (41) and hnRNPs (42), to exert its telomere-protective activity. Although the exact molecular mechanism of telomere protection by v5 still needs to be clarified, the central region present in the telomere-protective v5, but not in the nonprotective v2, should play a critical role in interacting with and/or regulating other factors yet to be identified. Given that a larger fraction of v5 was not colocalized with hRAP1 and TRF2 (Supplementary Fig. S10; data not shown) and that some telomere-binding proteins are suggested to function at other loci than telomeres (43), the investigation of a possible nontelomeric function of v5 will be also interesting.

The induction of cellular senescence by shRNA-mediated knockdown of endogenous v5 (Fig. 3), as well as the spontaneous down-regulation of endogenous v5 expression during replicative senescence (Supplementary Fig. S6), identified this POT1 variant as a novel, physiologic regulator of cellular senescence. The almost complete dependence of v5 knockdown-induced senescence on p53 response to DNA damage, in contrast to the efficient induction of senescence by v1 knockdown in the absence of a p53 response (Fig. 4*A–C*), highlighted the mechanistic difference between the roles of v1 and v5 in cellular senescence. The Western blot result showing p53 activation and $p16^{INK4A}$ up-regulation in senescent human fibroblasts with v1 knockdown (Fig. 4*D*) suggests that telomere dysfunction associated with the loss of 3′ overhangs in these cells triggered both the p53 and the $p16^{INK4A}$ DNA damage signaling pathways, as usually observed with telomere dysfunction-driven

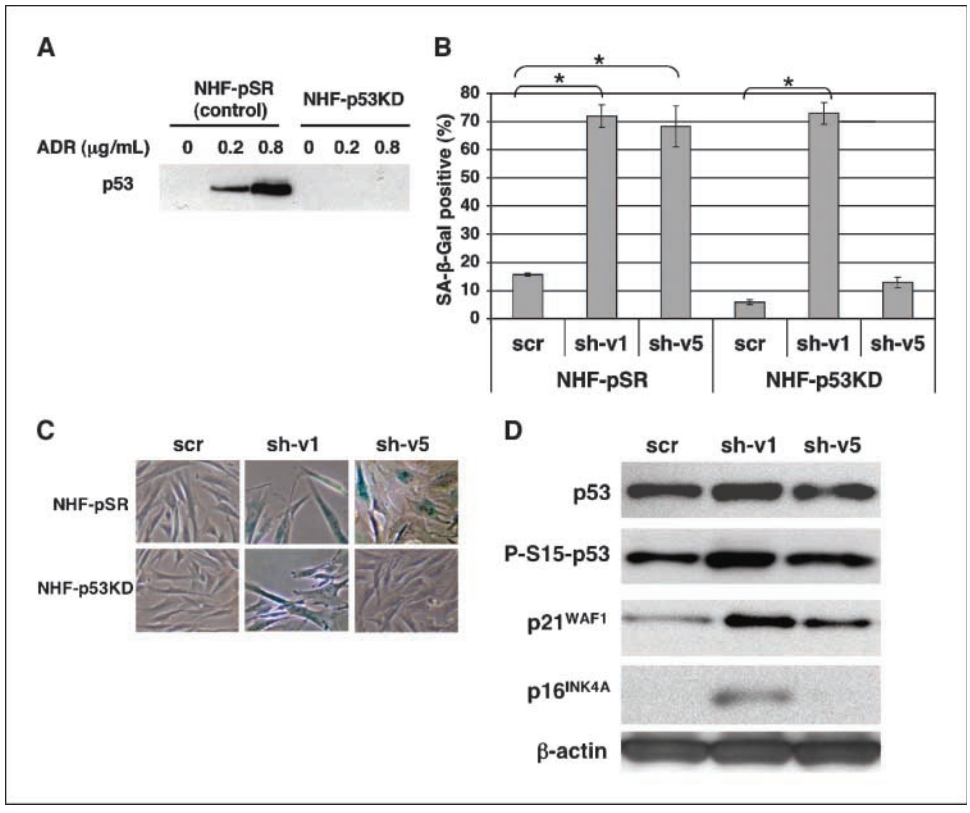

Figure 4. POT1v5 knockdown-induced senescence, but not POT1v1 knockdown-induced senescence, is abrogated in the absence of a p53 response. *A,* primary human NHF fibroblasts were transduced with a control vector (*NHF-pSR*) or shRNA knockdown vector targeting p53 (*NHF-p53KD*). The absence of a p53 response to Adriamycin (*ADR*) treatment (at indicated concentrations for 8 h) in NHF-p53KD was confirmed by Western blot. *B,* NHF-pSR and NHF-p53KD cells were transduced with scrambled shRNA control (*scr*), shRNA targeting POT1v1 (*sh-v1*), or shRNA targeting POT1v5 (*sh-v5*) and examined for SA-β-Gal activity, as performed in Fig. 3*A*. *Columns,* mean of three independent experiments; *bars,* SD. *, $P < 0.001$. *C,* representative pictures of SA-β-Gal staining. *D,* WI-38 fibroblasts transduced with control shRNA (*scr*), POT1v1 shRNA (*sh-v1*), or POT1v5 shRNA (*sh-v5*) were examined in Western blot for p53 (total amount), p53 phosphorylated at Ser^{15} residue (*P-S15-p53*), $p21^{WAF1}$, and $p16^{INK4A}$. β-Actin was a loading control.

senescence of human cells (44, 45). The increase in p53 phosphorylation and the up-regulation of $p21^{WAF1}$, without an increase in $p16^{INK4A}$, in senescent fibroblasts with v5 knockdown (Fig. 4*D*) are consistent with the p53 dependence of this senescence induction. Interestingly, mouse cell senescence induced by a *POT1a* deficiency (23) or overexpression of a mutant *POT1b* allele (21) was abrogated in the absence of p53, resembling human cell senescence induced by v5 knockdown. Mouse POT1 proteins may share a common mechanism for cellular senescence with human v5 variant.

There are some fundamental differences in telomere biology between mice and humans (46). Recent studies (21–23) showed that mice have two POT1 proteins (POT1a and POT1b) encoded by two

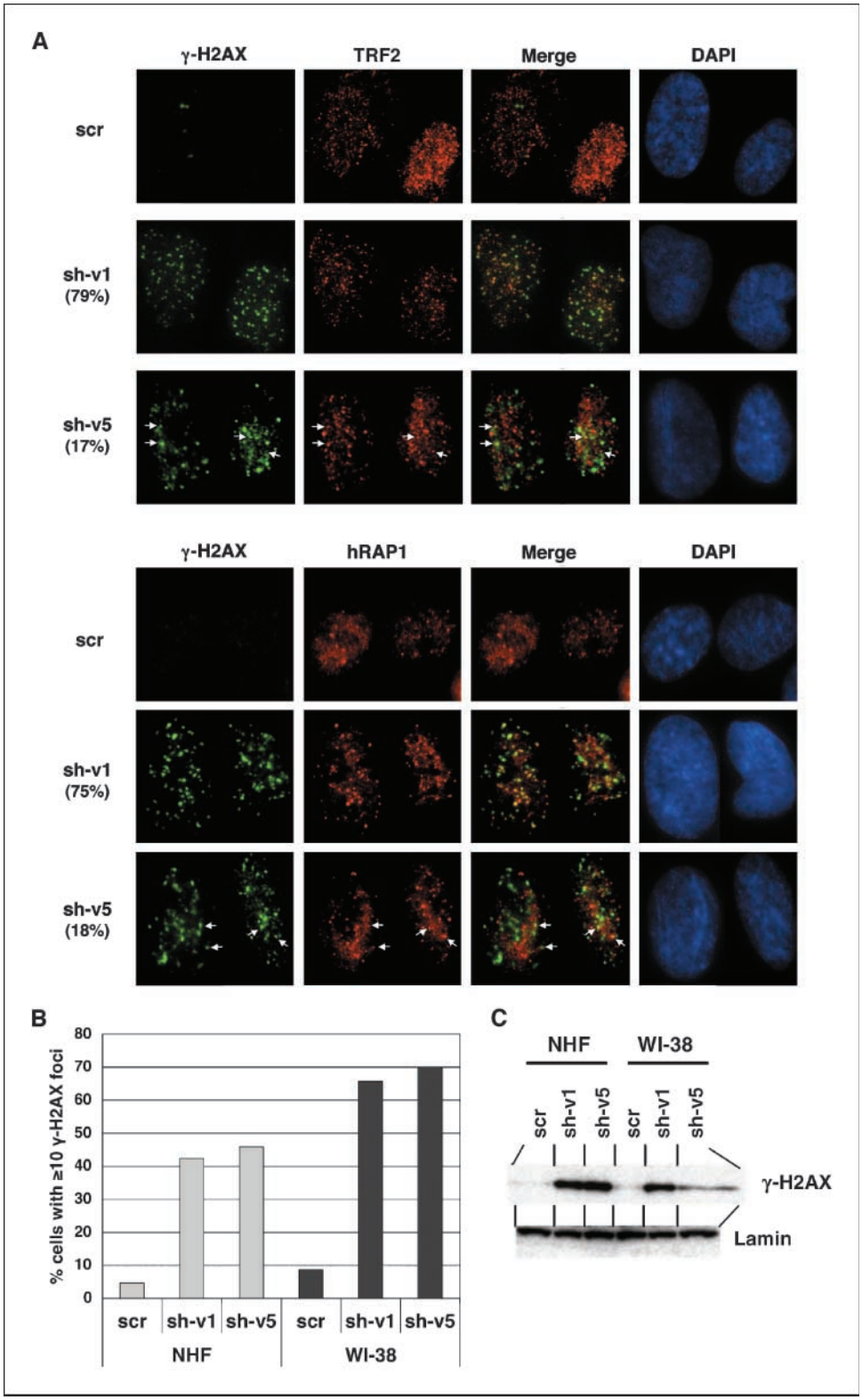

Figure 5. Differential formation of DNA damage foci in POT1v1 knockdown-induced versus POT1v5 knockdown-induced senescence. *A,* WI-38 fibroblasts transduced with scrambled shRNA control (*scr*), shRNA targeting POT1v1 (*sh-v1*), or shRNA targeting POT1v5 (*sh-v5*) were immunostained with anti-γ-H2AX mouse monoclonal antibody (*green*) together with anti-TRF2 antibody (*top*) or anti-hRAP1 antibody (*bottom*; *red*). The nuclei were counterstained with DAPI. The percentages of γ-H2AX foci that colocalize with TRF2 or hRAP1 signals (shown in the parentheses) were data from at least 10 cells. For sh-v5 cells, examples of the colocalization are indicated by *white arrows. B,* in NHF and WI-38 fibroblasts with control shRNA (*scr*), POT1v1 shRNA (*sh-v1*), or POT1v5 shRNA (*sh-v5*), the numbers of γ-H2AX foci were counted in at least 35 cells. The percentages of the cells with ≥10 γ-H2AX foci are graphed. *C,* the same set of shRNA-transduced cells as in *B* was examined for γ-H2AX levels in Western blot. Lamin A/C was a loading control.

Table 1. POT1v5 expression in MMR-proficient and MMR-deficient tumor tissues

Samples	MMR status*	POT1v5-positive/total cases examined†	
Colorectal cancer (HNPCC)	(−)	8/8	$P = 4.16E-12$‡
Colorectal cancer (sporadic)	(−)	10/10	
Colorectal cancer (sporadic)	(+)	1§/21	
Lung cancer	(+)	0/8	

*Determined by the National Cancer Institute–recommended panel of microsatellite markers. (+), MMR proficient; (−), MMR deficient.
† Determined by the RT-PCR as shown in Supplementary Fig. S11*B* and *C*.
‡ Fisher's exact probability test.
§ Case c1021 in Supplementary Fig. S11*C*.

different genes. POT1a and POT1b are functionally distinct, although they also have some redundant functions. Our findings that the variant forms of human POT1 protein produced from the single *POT1* gene have different biological activities on telomeres suggest a different mode of complexity in telomere regulation in humans from that in mice. Despite this genetic difference, human chromosome ends, like mouse ones, may also need at least two functionally distinct, telomere-protective POT1 isoforms (variants v1 and v5) for normal telomere function and DNA damage signaling. Considering the sequence similarity between human POT1v1 and mouse POT1 proteins (>70% identity), it may be surprising that they apparently have opposite effects on 3′ overhang regulation: *POT1a* deficiency (23) or *POT1b* deficiency (22) elongated 3′ overhang in mice, whereas decreased POT1v1 expression led to a reduction in 3′ overhang in humans (Figs. 2*C* and 3*B*; refs. 13, 14). Consistently, the overexpression of human POT1v1 caused an increase in 3′ overhang, which was resistant to the TRF2 inactivation-induced loss of 3′ overhang (Fig. 1*D*). Taken together with the elongation of 3′ overhang by *POT1* deletion in chicken cells (47) and the complete loss of telomeric DNA in *pot1*-deleted fission yeast (48), it is likely that, although POT1 proteins in various organisms are conserved structurally (i.e., OB fold) and functionally (i.e., control of DNA damage signaling at telomeres), they may have totally different effects on 3′ overhangs. Although the nature of this species-specific difference in 3′ overhang regulation is not known, the human POT1v1-specific protection of 3′ overhangs may be responsible for the ability to inhibit chromosome end-to-end fusions of human POT1v1 (Figs. 1*A* and *B* and 2*B*), which is modest but more significant than that of mouse POT1 proteins (22, 23).

The expression data in MMR-deficient and MMR-proficient cancer cells and tissues (Supplementary Fig. S11; Table 1) have implications in chromosome instability in human cancer. The correlation between v5 expression and MMR-deficient status suggests that a v5-specific function in telomere protection plays a role in maintaining chromosome stability observed in MMR-deficient human cancers. In the regions at and around the corresponding splicing donor and acceptor sites, there are no microsatellite repeats, which could be affected by MMR deficiency. We did not find somatic mutations in DNA sequences at and around those splicing sites in MMR-deficient and MMR-proficient cancer cell lines. The correction of MMR by chromosome transfer (26, 27) did not abrogate the v5 expression in otherwise MMR-deficient HEC59 and HCT116 cells (Supplementary Fig. S12), suggesting that MMR machinery itself does not regulate the alternative splicing. It is also unlikely that v5 plays a direct role in regulating the MMR activity, because the overexpression of v5 in MMR-proficient HT1080 cells did not induce microsatellite instability and the knockdown of v5 in MMR-deficient HEC59 cells did not correct the instability at BAT25 and D5S346 microsatellite loci (Supplementary Table S1). Further investigation will be needed to clarify what mechanism enhances the alternative splicing producing v5 mRNA.

Acknowledgments

Received 4/13/2007; revised 8/27/2007; accepted 9/24/2007.

Grant support: Finnish Cancer Society, Academy of Finland, and Sigrid Juselius Foundation. Part of this work was carried out at the Center of Excellence in Disease Genetics of the Academy of Finland (project number 44870). This research was also supported in part by the Intramural Research Program of the NIH, National Cancer Institute.

The costs of publication of this article were defrayed in part by the payment of page charges. This article must therefore be hereby marked *advertisement* in accordance with 18 U.S.C. Section 1734 solely to indicate this fact.

We thank Drs. Titia de Lange, Peter Baumann, Zhou Songyang, and Thomas Kunkel for reagents; Drs. Olga Sedelnikova, Olga Aprelikova, Eriko Michishita, Elisa Spillare, and Mohammed Khan for technical advice and expertise; Dr. Xin Wang for critical reading of the manuscript; Sini Marttinen for assistance; and Dorothea Dudek-Creaven for editorial assistance.

References

1. Griffith JD, Comeau L, Rosenfield S, et al. Mammalian telomeres end in a large duplex loop. Cell 1999;97:503–14.
2. de Lange T. Shelterin: the protein complex that shapes and safeguards human telomeres. Genes Dev 2005;19:2100–10.
3. Tahara H, Shin-Ya K, Seimiya H, Yamada H, Tsuruo T, Ide T. G-Quadruplex stabilization by telomestatin induces TRF2 protein dissociation from telomeres and anaphase bridge formation accompanied by loss of the 3′ telomeric overhang in cancer cells. Oncogene 2006;25:1955–66.
4. Stewart SA, Ben-Porath I, Carey VJ, O'Connor BF, Hahn WC, Weinberg RA. Erosion of the telomeric single-strand overhang at replicative senescence. Nat Genet 2003;33:492–6.
5. Maser RS, DePinho RA. Connecting chromosomes, crisis, and cancer. Science 2002;297:565–9.
6. Feldser DM, Hackett JA, Greider CW. Telomere dysfunction and the initiation of genome instability. Nat Rev Cancer 2003;3:623–7.
7. Blackburn EH. Telomeres and telomerase: their mechanisms of action and the effects of altering their functions. FEBS Lett 2005;579:859–62.
8. Lei M, Podell ER, Cech TR. Structure of human POT1 bound to telomeric single-stranded DNA provides a model for chromosome end-protection. Nat Struct Mol Biol 2004;11:1223–9.
9. Liu D, Safari A, O'Connor MS, et al. PTOP interacts with POT1 and regulates its localization to telomeres. Nat Cell Biol 2004;6:673–80.
10. Ye JZ, Hockemeyer D, Krutchinsky AN, et al. POT1-interacting protein PIP1: a telomere length regulator that recruits POT1 to the TIN2/TRF1 complex. Genes Dev 2004;18:1649–54.
11. Xin H, Liu D, Wan M, et al. TPP1 is a homologue of ciliate TEBP-β and interacts with POT1 to recruit telomerase. Nature 2007;445:559–62.
12. Wang F, Podell ER, Zaug AJ, et al. The POT1-TPP1 telomere complex is a telomerase processivity factor. Nature 2007;445:506–10.
13. Hockemeyer D, Sfeir AJ, Shay JW, Wright WE, de Lange T. POT1 protects telomeres from a transient DNA damage response and determines how human chromosomes end. EMBO J 2005;24:2667–78.
14. Yang Q, Zheng YL, Harris CC. POT1 and TRF2 cooperate to maintain telomeric integrity. Mol Cell Biol 2005;25:1070–80.
15. Veldman T, Etheridge KT, Counter CM. Loss of hPot1 function leads to telomere instability and a cut-like phenotype. Curr Biol 2004;14:2264–70.
16. Loayza D, de Lange T. POT1 as a terminal transducer of TRF1 telomere length control. Nature 2003;423:1013–8.
17. Lei M, Zaug AJ, Podell ER, Cech TR. Switching human telomerase on and off with hPOT1 protein *in vitro*. J Biol Chem 2005;280:20449–56.
18. Colgin LM, Baran K, Baumann P, Cech TR, Reddel RR. Human POT1 facilitates telomere elongation by telomerase. Curr Biol 2003;13:942–6.
19. Zaug AJ, Podell ER, Cech TR. Human POT1 disrupts telomeric G-quadruplexes allowing telomerase extension *in vitro*. Proc Natl Acad Sci U S A 2005;102:10864–9.

20. Opresko PL, Mason PA, Podell ER, et al. POT1 stimulates RecQ helicases WRN and BLM to unwind telomeric DNA substrates. J Biol Chem 2005;280: 32069–80.

21. He H, Multani AS, Cosme-Blanco W, et al. POT1b protects telomeres from end-to-end chromosomal fusions and aberrant homologous recombination. EMBO J 2006;25:5180–90.

22. Hockemeyer D, Daniels JP, Takai H, de Lange T. Recent expansion of the telomeric complex in rodents: two distinct POT1 proteins protect mouse telomeres. Cell 2006;126:63–77.

23. Wu L, Multani AS, He H, et al. Pot1 deficiency initiates DNA damage checkpoint activation and aberrant homologous recombination at telomeres. Cell 2006;126:49–62.

24. Baumann P, Podell E, Cech TR. Human Pot1 (protection of telomeres) protein: cytolocalization, gene structure, and alternative splicing. Mol Cell Biol 2002;22: 8079–87.

25. Sedelnikova OA, Horikawa I, Zimonjic DB, Popescu NC, Bonner WM, Barrett JC. Senescing human cells and ageing mice accumulate DNA lesions with unrepairable double-strand breaks. Nat Cell Biol 2004;6:168–70.

26. Koi M, Umar A, Chauhan DP, et al. Human chromosome 3 corrects mismatch repair deficiency and microsatellite instability and reduces *N*-methyl-*N*′-nitro-*N*-nitrosoguanidine tolerance in colon tumor cells with homozygous hMLH1 mutation. Cancer Res 1994;54: 4308–12.

27. Umar A, Koi M, Risinger JI, et al. Correction of hypermutability, *N*-methyl-*N*′-nitro-*N*-nitrosoguanidine resistance, and defective DNA mismatch repair by introducing chromosome 2 into human tumor cells with mutations in MSH2 and MSH6. Cancer Res 1997;57: 3949–55.

28. Michishita E, Park JY, Burneskis JM, Barrett JC, Horikawa I. Evolutionarily conserved and nonconserved cellular localizations and functions of human SIRT proteins. Mol Biol Cell 2005;16:4623–35.

29. Brummelkamp TR, Bernards R, Agami R. A system for stable expression of short interfering RNAs in mammalian cells. Science 2002;296:550–3.

30. van Steensel B, Smogorzewska A, de Lange T. TRF2 protects human telomeres from end-to-end fusions. Cell 1998;92:401–13.

31. Horikawa I, Cable PL, Mazur SJ, Appella E, Afshari CA, Barrett JC. Downstream E-box-mediated regulation of the human telomerase reverse transcriptase (hTERT) gene transcription: evidence for an endogenous mechanism of transcriptional repression. Mol Biol Cell 2002; 13:2585–97.

32. Miura N, Horikawa I, Nishimoto A, et al. Progressive telomere shortening and telomerase reactivation during hepatocellular carcinogenesis. Cancer Genet Cytogenet 1997;93:56–62.

33. Rogakou EP, Boon C, Redon C, Bonner WM. Megabase chromatin domains involved in DNA double-strand breaks *in vivo*. J Cell Biol 1999;146:905–16.

34. Sinha-Datta U, Horikawa I, Michishita E, et al. Transcriptional activation of hTERT through the NF-κB pathway in HTLV-I-transformed cells. Blood 2004; 104:2523–31.

35. Salovaara R, Loukola A, Kristo P, et al. Population-based molecular detection of hereditary nonpolyposis colorectal cancer. J Clin Oncol 2000;18:2193–200.

36. Aaltonen LA, Salovaara R, Kristo P, et al. Incidence of hereditary nonpolyposis colorectal cancer and the feasibility of molecular screening for the disease. N Engl J Med 1998;338:1481–7.

37. Smogorzewska A, van Steensel B, Bianchi A, et al. Control of human telomere length by TRF1 and TRF2. Mol Cell Biol 2000;20:1659–68.

38. Bodnar AG, Ouellette M, Frolkis M, et al. Extension of life-span by introduction of telomerase into normal human cells. Science 1998;279:349–52.

39. Li B, Oestreich S, de Lange T. Identification of human Rap1: implications for telomere evolution. Cell 2000;101: 471–83.

40. Lengauer C, Kinzler KW, Vogelstein B. Genetic instability in colorectal cancers. Nature 1997;386:623–7.

41. Salas TR, Petruseva I, Lavrik O, et al. Human replication protein A unfolds telomeric G-quadruplexes. Nucleic Acids Res 2006;34:4857–65.

42. LaBranche H, Dupuis S, Ben-David Y, Bani MR, Wellinger RJ, Chabot B. Telomere elongation by hnRNP A1 and a derivative that interacts with telomeric repeats and telomerase. Nat Genet 1998;19: 199–202.

43. Bradshaw PS, Stavropoulos DJ, Meyn MS. Human telomeric protein TRF2 associates with genomic double-strand breaks as an early response to DNA damage. Nat Genet 2005;37:193–7.

44. Smogorzewska A, de Lange T. Different telomere damage signaling pathways in human and mouse cells. EMBO J 2002;21:4338–48.

45. Jacobs JJ, de Lange T. Significant role for p16INK4a in p53-independent telomere-directed senescence. Curr Biol 2004;14:2302–8.

46. Rangarajan A, Weinberg RA. Comparative biology of mouse versus human cells: modelling human cancer in mice. Nat Rev Cancer 2003;3:952–9.

47. Churikov D, Wei C, Price CM. Vertebrate POT1 restricts G-overhang length and prevents activation of a telomeric DNA damage checkpoint but is dispensable for overhang protection. Mol Cell Biol 2006;26: 6971–82.

48. Baumann P, Cech TR. Pot1, the putative telomere end-binding protein in fission yeast and humans. Science 2001;292:1171–5.